Observation of Coherence and Partial Decoherence of Quantized Spin Waves in Nanoscaled Magnetic Ring Structures

H. Schultheiss, S. Schäfer, P. Candeloro, B. Leven, and B. Hillebrands
Fachbereich Physik and Forschungsschwerpunkt MINAS, Technische Universität Kaiserslautern, D-67663 Kaiserslautern, Germany

A. N. Slavin
Department of Physics, Oakland University, Rochester, Michigan 48309, USA
(Received 10 September 2007; published 31 January 2008)

Experiments and simulations are reported, which demonstrate the influence of partial decoherence of spin-wave modes on the dynamics in small magnetic structures. Microfocus Brillouin light scattering spectroscopy was performed on 15 nm thick $Ni_{81}Fe_{19}$ rings with diameters from 1 to 3 μm. For the so-called "onion" magnetization state several effects were identified. First, in the pole regions of the rings spin-wave wells are created due to the inhomogeneous internal field leading to spin-wave confinement. Second, in the regions in between, modes are observed which show a well pronounced quantization in radial direction but a transition from partial to full coherency in azimuthal direction as a function of decreasing ring size. In particular for larger rings a continuous frequency variation with position is observed which is well reproduced by spin-wave calculations and micromagnetic simulations.

DOI: 10.1103/PhysRevLett.100.047204 PACS numbers: 75.30.Ds, 75.40.Gb

The topic of magnetization dynamics in small magnetic structures, such as stripes [1], rectangles [2], disks and rings [3–8], has been widely investigated using a variety of experimental techniques. Most often, the determination and the understanding of the spin-wave eigenmode spectrum was in the focus of interest. Eigenmodes in confined objects form standing spin-wave patterns. It is evident that they exist if the coherence length of the spin wave is larger than the dimensions of the confining structure in order to allow for a standing wave pattern to form. Often, the boundaries of a small magnetic structure cause such a mode confinement. Inhomogeneous internal magnetic fields are a further source of confinement due to the formation of regions with allowed and forbidden spin-wave propagation [2]. Surprisingly, effects of finite coherence length have been little addressed so far. Here we report on experiments on fully and partially coherent spin-wave modes, and we demonstrate the transition from coherence to partial decoherence. We use the richness of spin-wave modes in magnetic rings to address this issue since the mode spectrum in these structures provides an excellent experimental testing ground for the problems addressed here.

An eigenmode of a magnetic structure is characterized by a unique frequency, i.e., energy eigenvalue. As the internal field is most often inhomogeneous across a structure, the spin-wave wave vector is known to spatially adapt to the local internal field [2]. A true eigenmode of a system is dissipationless by definition (which is an approximation working sufficiently well for permalloy considered here) and fully coherent. It must fulfill the phase quantization condition

$$\int k[H(z), \nu]dz = r\pi, \tag{1}$$

where $r = 1, 2, 3, \ldots$ and the wave vector k is determined by the eigenmode frequency ν and the value of the internal field H at position z according to the spin-wave dispersion relation.

Each eigenmode is characterized by a characteristic spatial distribution of the mode amplitude. In case of loss of coherence the frequency quantization condition Eq. (1) will not hold anymore and mode broadening is expected.

In this Letter we report on investigations of thermally activated spin waves in several ring-shaped magnetic microstructures with varying degrees of confinement using the newly developed microfocus Brillouin light scattering (BLS) spectroscopy technique [9,10]. For this purpose,

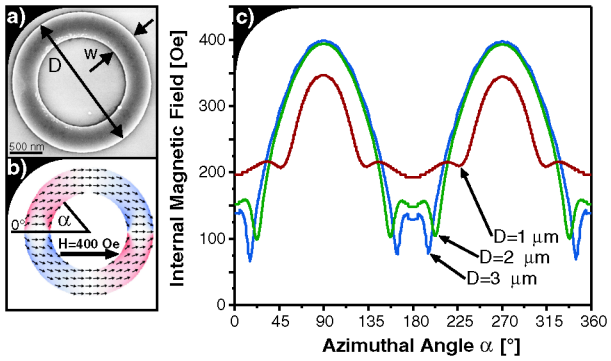

FIG. 1 (color online). (a) Scanning electron microscopy image of a permalloy ($Ni_{81}Fe_{19}$) ring structure with diameter $D = 2$ μm and width $w = 400$ nm prepared by molecular beam epitaxy and electron beam lithography. (b) Onion state configuration of the magnetization calculated with OOMMF for a ring with $D = 2$ μm, $w = 400$ nm, and an externally applied field of $H = 400$ Oe. (c) Distribution of the internal magnetic field along a path with a radius $R = D/2 - w/2$ for $D = 1$, 2, and 3 μm and a constant width $w = 400$ nm.

permalloy ($Ni_{81}Fe_{19}$) rings with outer diameters of $D = 1$, 2, and 3 μm, ring widths of $w = 400$ nm, and thicknesses of 15 nm were prepared by molecular beam epitaxy in an UHV system and subsequent electron beam lithography, utilizing a lift-off technique; see Fig. 1(a) for a corresponding scanning electron microscopy image. One possible magnetic configuration of such rings is the so-called "onion state," which is depicted in Fig. 1(b) for a ring with an outer diameter of $D = 2$ μm, a width of $w = 400$ nm, and an externally applied in-plane field of $H = 400$ Oe in horizontal direction [see inset of Fig. 1(b)]. A characteristic property of this magnetization state is the inhomogeneity of the internal field along the ring perimeter. Micromagnetic simulations, performed by means of the OOMMF code [11], were carried out to calculate the internal field along the ring for all three types of rings studied. The results of these simulations are plotted in Fig. 1(c), which shows the internal field as a function of the azimuthal angle α used as the space coordinate, as indicated in Fig. 1(b). In all three cases the internal field varies with position, and it is reduced in the pole regions (at $\alpha = 0°$ and 180°), caused by a nonzero magnetization component perpendicular to the ring perimeter. In the equatorial regions (i.e., at $\alpha = 90°$ and 270°) the magnetization is aligned parallel to the ring perimeter, and the internal field is nearly equal to its external counterpart.

Several spin-wave modes are considered: (i) modes traveling about the ring forming a standing wave about the entire ring (so-called longitudinal quantization), (ii) modes forming a standing wave between the inner and outer perimeter of the ring (so-called transverse quantization), and (iii) modes confined to the pole regions due to the low internal field causing confinement.

Spin-wave modes are investigated using microfocus Brillouin light scattering spectroscopy. This technique allows for the determination of local magnetic excitation spectra with a spatial resolution of better than 300 nm and a frequency resolution of up to 0.1 GHz [9,10]. In the experiments spectra have been taken along the ring varying the azimuthal angle α. The results are shown in Figs. 2(a)–2(c) for ring diameters of 1, 2, and 3 μm, respectively. In each case, the anti-Stokes sides of the spectra are plotted as vertical lines in gray-scale code as a function of α. Examples for individual spectra measured at $\alpha = 90°$ are given in 2(d)–2(f), corresponding to cross sections of the gray-scale maps in the equatorial region.

Figure 2 clearly demonstrates that various spin-wave modes are excited. Inspecting the results as a function of the ring diameter D, it is evident that the ring with the smallest diameter ($D = 1$ μm) shows well resolved, discrete spin-wave modes, whereas the ring with the largest diameter ($D = 3$ μm) shows a continuous variation of the frequencies as a function of α. Evidently we observe here the transition from fully coherent to incoherent modes. The $D = 2$ μm ring exhibits an intermediate case. Overall, all

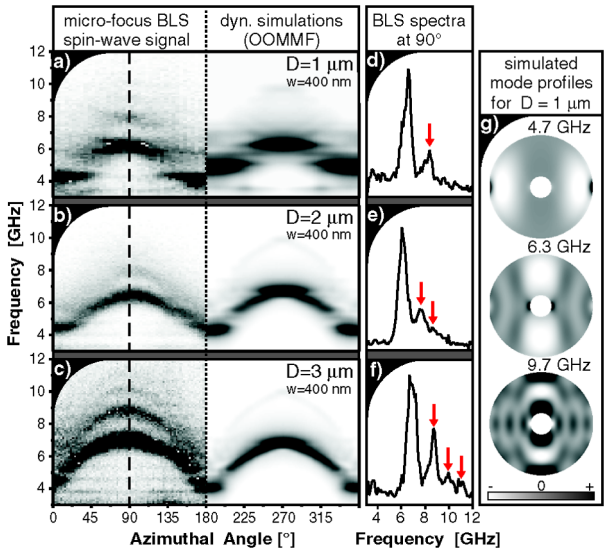

FIG. 2 (color online). (a)–(c) The left half of the gray-scale maps represents the microfocus BLS spectra for rings with outer diameters of 1 (a), 2 (b), and 3 μm (c), respectively, and a constant width of 400 nm as a function of the azimuthal angle. Dark shades correspond to high spin-wave amplitudes. In the right half of the panels the results of the micromagnetic simulations are displayed. (d)–(f) BLS spectra measured in the equatorial region at $\alpha = 90°$. Higher modes which are discussed in the text are marked with arrows. (g) Simulated amplitudes for the most significant eigenmodes of the 1 μm ring in panel (a) using the OOMMF code. Black and white indicate positive and negative spin-wave amplitude as indicated by the gray-scale bar.

modes roughly follow the local value of the internal field, although with discrete jumps for the $D = 1$ μm ring. For the smallest ring, the results indicate the presence of a fully coherent eigenmode system in agreement with recent works [4–8]. Obviously, and discussed in more detail below, longitudinal quantization takes place for the smallest ring, but not for the largest ring studied here. The observed set of modes for each sample and each angle α can be attributed to radial quantization due to the finite width $w = 400$ nm of the rings.

These conclusions are supported by the results of micromagnetic simulations. The dynamic response of the rings after a short field pulse (0.01 ns) with a small amplitude (1 Oe) perpendicular to the static external field of 400 Oe was simulated using the OOMMF code. For the simulations a value of 650 G for the saturation magnetization M_s (smaller than the literature value for $Ni_{81}Fe_{19}$ due to reasons discussed below), an exchange stiffness of $A = 1.6 \times 10^{-6}$ erg/cm, and a gyromagnetic ratio of $\gamma = 1.76 \times 10^{-2}$ GHz/Oe were used. A damping constant $\alpha = 0.01$ typical for permalloy was assumed. The simulations yield the time evolution of the magnetization inside the ring. These data are Fourier-transformed point by point to the frequency domain. In the right half of panels (a–c) of Fig. 2 the intensities of the Fourier transformations are

displayed as a function of the azimuthal angle and the frequency in a gray-scale plot, analogous to the presented BLS spectra. To take into account the finite spatial resolution of the experiment we convoluted the simulated spin-wave amplitudes with a two-dimensional Gaussian function with 300 nm FWHM. As it can be seen from Fig. 2, an excellent agreement between the simulation results and the experimentally obtained data is achieved. Because of the uniform spatial distribution of the pulse only radial modes with an odd quantization number can be excited [12]. Therefore, the even order modes observed in the experiment cannot be seen in the simulations. Figure 2(g) shows the simulated spatial distribution of the most significant modes of the 1 μm ring observable in the gray-scale maps. The profile of the lower frequency mode (6.3 GHz) located in the equatorial region exhibits no node, while two nodes in radial direction are present for the corresponding higher mode (9.7 GHz). This is a clear indication that the higher modes observed in the experiment are due to quantization effects along the radial direction.

Although the numerical simulations provide already a good account for the observed experimental phenomena, a theoretical analysis allows for deeper insight. For the ring with $D = 3$ μm, calculations based on the spin-wave dispersion equation for thin films [13] were performed. The results are shown in Fig. 3 and can be understood as follows. In the equatorial region, where the frequencies are changing continuously, the ring structure is approximated by an infinitely extended stripe aligned tangentially to the ring, as shown schematically in Fig. 4(a) by the red boxes. The quantization in radial direction is modeled by an infinitely extended stripe of same width as the ring. Taking into account the effective dipolar pinning [14] of the spin waves at the lateral edges of the stripe, the effective width w_{eff} to be considered is 440 nm. Because of the lack of boundary conditions along the long axis of the stripe no quantization of the azimuthal wave vector in the equatorial region is included in the calculation. The quantization in radial direction is accounted for by the following expression: $k_r = n\pi/w_{\mathrm{eff}}$, where k_r is the radial wave vector component, $n \in \mathbb{N}$, and $n \neq 0$, since a uniform mode is not allowed due to the effective dipolar pinning at the ring boundaries. It has been shown that the frequency dispersion of the spin waves in confined magnetic elements can be described by the dispersion for an infinite in-plane magnetized film in first approximation by [13,15]

$$\nu_0^2(k) = \frac{\gamma^2}{4\pi^2}\left(H_{\mathrm{int}} + \frac{2A}{M_s}k^2\right) \times \left(H_{\mathrm{int}} + \frac{2A}{M_s}k^2 + 4\pi M_s F_{00}(k)\right), \qquad (2)$$

where the matrix element $F_{00}(k, \theta)$ of the dipole-dipole interaction given in [13] is a function of the relative angle θ_k between the local static magnetization and the local wave vector.

If we only assume wave vectors in radial direction, the angle between the wave vector and the magnetization is changing continuously as a function of position along the ring [Fig. 4(b)]. In order to determine the dependence of θ on the azimuthal angle α, the equilibrium magnetic configuration of a ring with $D = 3$ μm in an external field of 400 Oe was calculated using the OOMMF code. The direction of magnetization varies between perpendicular and parallel to the perimeter between the pole and the equatorial regions. Inspecting Eq. (2) we find that the spin-wave frequency is very sensitive not only to the value of the internal field but also to θ. The latter is due to the fact that the spin-wave character is continuously varying from Damon-Eshbach-like to backward volume-like spin-waves. Evaluation of Eq. (2) yields the dependence of the frequency on α for the different radial modes. The results of these calculations are plotted for the equatorial region as continuous lines in Fig. 3. The only fitting parameter here is the saturation magnetization, yielding a

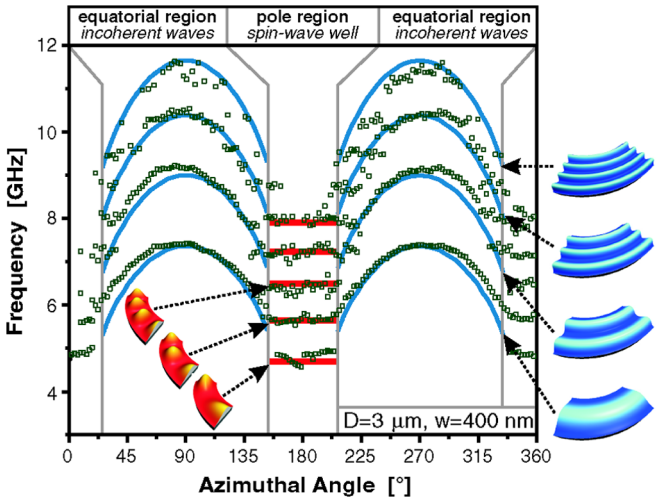

FIG. 3 (color online). Fitted spin-wave frequencies as a function of the azimuthal position in the $D = 3$ μm ring with an external field of 400 Oe. The lines represent the calculations for the different ring segments.

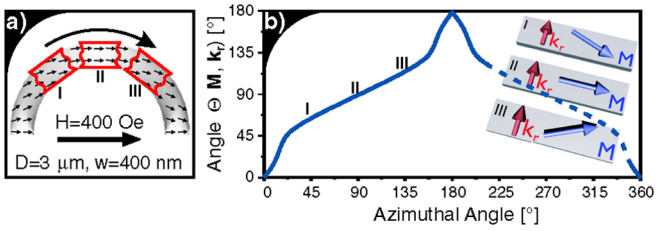

FIG. 4 (color online). (a) Schematic illustration of the approximation of a ring structure by infinitely extended stripes. (b) Dependence of the angle θ between magnetization and radial wave vector k_r on the azimuthal angle α, calculated by OOMMF. The inset schematically illustrates the configurations at the locations I–III in panel (a).

value of $M_s = 650$ G. This value is noticeably smaller than the literature value of 860 G. The reason is heating of the sample in the laser spot, which cannot be fully avoided due to low cross section reasons. The very small laser spot size in a microfocus BLS experiment demands for a significantly higher light intensity in the laser spot region. The excellent agreement of the calculations with the experimental results (Fig. 3) substantiates the existence of spin waves, which are incoherent in azimuthal direction within the equatorial region for the 3 μm ring.

A closer look at the spin-wave frequencies of the 3 μm ring in Fig. 3 reveals additional features of the magnetization dynamics. In narrow angular sections around the poles several modes with constant frequencies can be observed. Their frequency spacing differs from the resonances found in the equatorial region, thus indicating that their discretization is not due to confinement in radial direction. These modes correspond to spin waves trapped in so-called ''spin-wave wells'' formed by the spatial inhomogeneity of the internal field, as shown in Fig. 1(c). This quantization mechanism was first observed in perpendicularly magnetized stripes [2] and occurs due to a field-induced shift of the spin-wave frequencies into regions where no real wave vector exists. In Fig. 3 the experimental data are shown together with calculations for the spin-wave frequencies in this ring section. Around the pole position the ring was approximated by a rectangular element with lateral sizes of 440 nm and 1180 nm in radial and azimuthal direction, respectively. The length of this element corresponds to the effective length of the spin-wave well and is assumed to be constant for all the modes in the pole region in first approximation, due to the abrupt change of the internal field. Despite this approximation, the calculated frequencies for higher modes in azimuthal direction are in good agreement with the measured data.

In conclusion spin-wave quantization in small magnetic rings magnetized in the onion state with different diameters was investigated by means of microfocus BLS. In the case of the smallest ring with a diameter of 1 μm, a two-dimensional quantization in radial and azimuthal direction was found, whereas loss of coherence of the spin waves in azimuthal direction was observed for the rings with larger diameter. In order to calculate the continuously changing spin-wave frequencies in the 3 μm ring a simple model was developed using an infinitely extended stripe aligned tangentially to the ring structure. Within the frame of this approximation both the inhomogeneous magnetization distribution and the variation of the internal field were taken into account. Moreover, numerical simulations of the magnetization dynamics carried out by means of OOMMF are in very good agreement with the experimental data for all the investigated ring geometries. Thus, taking finite coherence into account, the spin-wave mode spectrum in a small magnetic ring can be well understood.

Support by the Priority Program No. SPP 1133 of the Deutsche Forschungsgemeinschaft and the NEDO International Joint Research Program No. 2004IT093, Japan, is gratefully acknowledged.

[1] S. O. Demokritov, B. Hillebrands, and A. N. Slavin, Phys. Rep. **348**, 441 (2001).
[2] J. Jorzick, S. O. Demokritov, B. Hillebrands, M. Bailleul, C. Fermon, K. Y. Guslienko, A. N. Slavin, D. V. Berkov, and N. L. Gorn, Phys. Rev. Lett. **88**, 047204 (2002).
[3] X. Zhu, M. Malac, Z. Liu, H. Qian, V. Metlushko, and M. R. Freeman, Appl. Phys. Lett. **86**, 262502 (2005).
[4] F. Giesen, J. Podbielski, T. Korn, and D. Grundler, J. Appl. Phys. **97**, 10A712 (2005).
[5] J. Podbielski, F. Giesen, and D. Grundler, Phys. Rev. Lett. **96**, 167207 (2006).
[6] I. Neudecker *et al.*, Phys. Rev. Lett. **96**, 057207 (2006).
[7] G. Gubbiotti, M. Madami, S. Tacchi, G. Carlotti, H. Tanigawa, T. Ono, L. Giovannini, F. Montoncello, and F. Nizzoli, Phys. Rev. Lett. **97**, 247203 (2006).
[8] M. Buess, R. Höllinger, T. Haug, K. Perzlmaier, U. Krey, D. Pescia, M. R. Scheinfein, D. Weiss, and C. H. Back, Phys. Rev. Lett. **93**, 077207 (2004).
[9] V. E. Demidov, S. O. Demokritov, B. Hillebrands, M. Laufenberg, and P. P. Freitas, Appl. Phys. Lett. **85**, 2866 (2004).
[10] K. Perzlmaier, M. Buess, C. H. Back, V. E. Demidov, B. Hillebrands, and S. O. Demokritov, Phys. Rev. Lett. **94**, 057202 (2005).
[11] M. J. Donahue and D. G. Porter, National Institute of Standards and Technology Report No. NISTIR 6376, 1999.
[12] M. Bolte, G. Meier, and C. Bayer, Phys. Rev. B **73**, 052406 (2006).
[13] B. A. Kalinikos and A. N. Slavin, J. Phys. C **19**, 7013 (1986).
[14] K. Y. Guslienko, S. O. Demokritov, B. Hillebrands, and A. N. Slavin, Phys. Rev. B **66**, 132402 (2002).
[15] C. Bayer *et al.*, Phys. Rev. B **72**, 064427 (2005).